Detection of metastatic liver tumor in multi-phase CT images by using a spherical gray-level differentiation searching filter

Xuejun Zhang[*a,b], Takahiro Furukawa[a], Xiangrong Zhou[a], Takeshi Hara[a], Masayuki Kanematsu[c], Hiroshi Fujita[a]

[a] Department of Intelligent Image Information, Division of Regeneration and Advanced Medical Sciences, Graduate School of Medicine, Gifu University, Gifu 501-1194, Japan
[b] School of Computer, Electronics and Information, Department of Electronics and Information Engineering, Guangxi University, Nanning City, Guangxi 530004, P. R. China
[c] Department of Radiology, Gifu University School of Medicine & Gifu University Hospital, Gifu 501-1194, Japan

ABSTRACT

To detect the metastatic liver tumor on CT scans, two liver edge maps on unenhanced and portal venous phase images are firstly extracted and registered using phase-only correlation (POC) method, by which rotation and shift parameters are detected on two log-polar transformed power spectrum images. Then the liver gray map is obtained on non-contrast phase images by calculating the gray value within the region of edge map. The initial tumors are derived from the subtraction of edge and gray maps as well as referring to the score from the spherical gray-level differentiation searching (SGDS) filter. Finally the FPs are eliminated by shape and texture features. 12 normal cases and 25 cases with 44 metastatic liver tumors are used to test the performance of our algorithm, 86.7% of TPs are successfully extracted by our CAD system with 2.5 FPs per case. The result demonstrates that the POC is a robust method for the liver registration, and our proposed SGDS filter is effective to detect spherical shape tumor on CT images. It is expected that our CAD system could useful for quantitative assessment of metastatic liver tumor in clinical practice.

Keywords: Segmentation, Liver, Metastatic tumor, Multi-phase CT, Gray-level differentiation searching (SGDS) filter, Computer-aided diagnosis

1. INTRODUCTION

The liver is the largest organ in the body, and it involves almost all the biochemical pathways that function in allowing growth, fighting disease, supplying nutrients, providing energy, and aiding reproduction. Of the total blood pumped out with each heartbeat, 25% reaches the liver; in fact, the liver receives blood from two blood vessels—the portal vein and the hepatic artery. This additional blood supply facilitates the spread of metastatic tumors present in other organs into the liver. Cancer may develop directly in the liver (primary) or spread from other sites (metastatic or secondary) via the circulatory or lymphatic systems. Malignant liver tumor such as hepatocellular carcinoma (HCC) or metastatic liver tumor causes 1.25 million deaths per year worldwide [1]. Currently, surgery, either by resection (removal of the tumor) or liver transplantation, offers the only chance to cure liver cancers. By now the Multidetector CT (MDCT) is currently an effective diagnostic modality for the detection, characterization of liver tumors, as well as a powerful image source for surgical planning. However, the interpretation of large number of images is a huge burden for the radiologists. We have been developing several computer aided diagnosis (CAD) systems for liver that are proven to be able to improve the accuracy of clinical diagnosis and efficiency of surgical resection [2-5]. This paper is to describe our novel method on the detection of metastatic liver tumor on CT scans.

There are some studies on the extraction of hepatic tumor by computer algorithms. Tajima [6] presents their edge detection and subtraction processing based method for detecting HCC, which is indicated by high- and low-intensity regions on CT scans in arterial and equilibrium phase images, respectively. Within a segmented liver area, black regions were selected by subtracting the equilibrium phase images with the corresponding registered arterial phase images. From these black regions, the HCC candidates were extracted as the areas without edges by using Sobel and LoG edge

* Email: xjzhang@gxu.edu.cn; phone 81 58 230-6513; fax 81 58 230-6514

Medical Imaging 2011: Computer-Aided Diagnosis, edited by Ronald M. Summers, Bram van Ginneken,
Proc. of SPIE Vol. 7963, 79632K · © 2011 SPIE · CCC code: 0277-786X/11/$18 · doi: 10.1117/12.878379

detection filters. The FP candidates were eliminated by using 6 features extracted from the cancerous and the surrounding liver regions. Finally, an expansion process was applied to acquire the 3D shape of the HCC. Due to the presence of some unclear HCC, this method is effective to detect subtle tumors. However the high- and low-intensity pattern is not observed in the metastatic liver tumor, therefore the above method cannot be used in this study. Xu[7] develops a suitable image registration algorithm to align the two volumes in order to transform the tumors in the preoperative volumes to the MR volumes to assist in MR-guided interventional therapy. Their result shows that the non-rigid registration method is sufficiently accurate for the coagulation of liver tumors. Freiman [8] proposes an automatic detection method for computer aided early detection of liver metastases. The method used fMRI-based statistical modeling to characterize colorectal hepatic metastases and follow their early hemodynamical changes. A classification model was built to differentiate between metastatic and healthy liver tissue. The model is constructed from 128 validated fMRI samples of metastatic and healthy mice liver tissue using histogram-based features and SVM classification engine. The model yields an accuracy of 84.38% with 80% precision. Differing from these two MR studies, metastatic liver tumors often show low absorption to liver area on CT in both non-contrast phase and portal phase with spherical shape. We proposed a spherical gray-level differentiation searching (SGDS) filter to find out the tumors candidate according to these two features.

2. MERTIERALS AND METHODS

A brief flowchart of metastatic tumor segmentation on CT images is shown in Figure 1. Our method consists three main steps: (1) Extraction of the liver edge maps on unenhanced and portal venous phase images and registration by phase-only correlation (POC), (2) Detection of the liver gray maps on non-contrast phase images and obtain the initial tumors from subtraction of edge maps with the output score of SGDS filter, (3) Eliminating the FPs and classification of tumors into benign and malignant according to different attenuation values from other phase images.

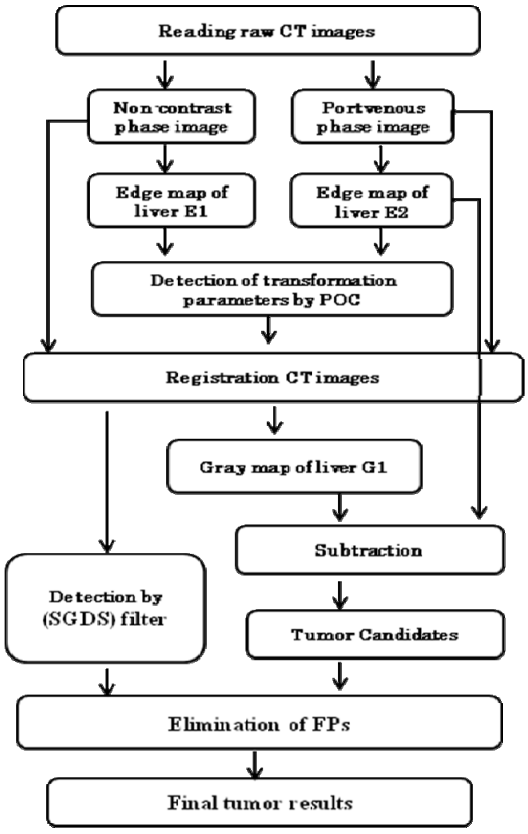

Figure 1. A brief flowchart of metastatic tumor segmentation on CT images.

2.1 Materials

Datasets were examined with different multi-detector row CT scanners ((LightSpeed Ultra of GE Healthcare or Aquilion of TOSHIBA) that included unenhanced and portal venous images. Each patient received the contrast/bolus agent (Oypalomin370 or Optiray320) via a power injector at a rate of 3 ml/s, and the final average volume of contrast material was 100 ml (range, 110–182 ml), with slice interval, 0.625–1.25 mm; bits stored, 16 bits; pixel-spacing, 0.50–0.625 mm; spatial resolution, 512 × 512; 165 mAs; and 120 kVp. These cases were categorized by experienced radiologists with 12 normal cases, 25 cases with 44 metastatic liver tumor confirmed.

2.2 Extraction of the liver edge maps and registration by POC

Fully segmentation of liver region with tumorous tissues is a challenge task as the liver tissues have a wide distribution of intensity and standard deviation in different CT images that are acquired by different modalities or parameter settings. Therefore, it is difficult to automatically determine a proper grey value as the threshold for binarization so as to keep the tumor inside the liver map. We propose a method by using edge processing to overcome these problems [9, 10]. By combining the Sobel and LoG filters, we can extract the subtle edges that maybe undetected when each method is used individually. After edge detection, the region of hepatic tissues as well as most of the tumor tissues are turned into black and only remain a closed contour along liver surface. The initial liver region, which is separated into one of the dark labels on edge map, can be picked up as the largest 3D label in the abdominal CT images except for the background. Two liver edge maps are provided by our non-intensity based edge-detection method on non-contrast and portal venous phase images as shown in Fig. 2(a) and (b). Mean gray values within the edge map are calculated as a reference threshold value and two gray liver maps are derived by binarization processing.

As the two sequenced images are scanned in a continuous time, the transformation of two liver maps is mainly rigid: rotation and displacement alignment. Our image registration algorithm based on phase-only correlation (POC) [11] is applied to the two liver edge maps to detect translational shift. Generally the magnitude and the phase obtained by Fast Fourier transform (FFT) can completely describe a function in the frequency domain. Sometimes, only information regarding the magnitudes is considered, such as the power spectrum, where phase information is completely ignored. However when the targets are focused on the shape, edge or position, the phase information is considered more important than the magnitude in an image pattern. The phase-only correlation of image ***g*** and ***h*** is defined as:

$$\mathrm{POC}_{g,h}(x, y) = F^{-1}\{G(u, v)H(u, v)^*\}/|G(u, v)H(u, v)^*|$$

The POC function is very similar to the calculation of correlation between two images in the frequency domain, while a main difference is that it is divided by two normalization factors. This change produces a sharper correlation peak on POC image even if the targets in two images have different shift or scale but with same shape. Therefore the POC method has the advantage of shift, scale and brightness invariance as magnitude is unity throughout the spectrum. However it is not rotation invariance when applying the POC to the images shown in Fig.2 (a) and (b), that may be a

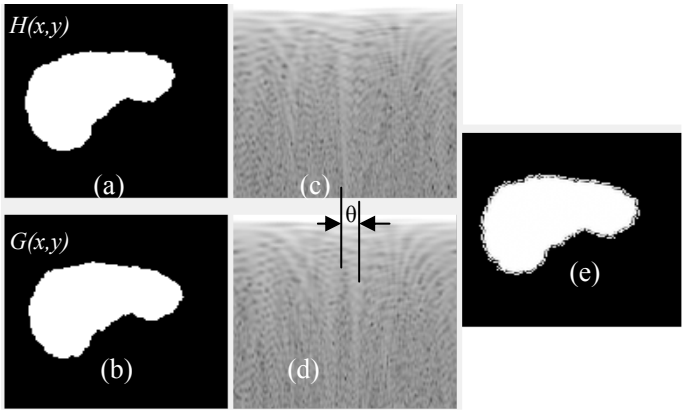

Figure 2. Registration result from the liver edge maps on unenhanced (a) to the portal venous phase (b) images with a largest liver slice. The power spectra of two map images are firstly calculated from FFT and then transformed into polarized coordinate in (c) and (d), respectively. Calculating the shift between (c) and (d) by POC method, θ is calculated as the rotation angle from which a registered image (e) is derived, corresponding to image (a). Therefore, rotation is turned into shift problem.

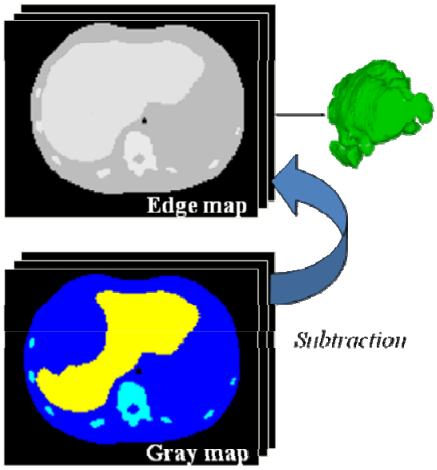

Figure 3. Large tumor candidates with radius more than 10 mms are extracted by using the subtraction result image on edge map and gray map as the tumor region is exist in an edge liver map while inexistence in a gray liver map.

limitation to the registration performance. In our experiment, the power spectrum of two average liver map derived from our previous method [9] are firstly calculated by FFT (fast Fourier transform) and then transformed into polarized coordinate by log-polar transform [12] as shown in Fig. 2(c) and (d), from which the POC is applied to determine the horizontal shift of the power spectrum images, that equal to the rotation angle θ in spatial domain. Secondary the non-contrast average liver map is rotated by θ to keep the same direction with portal venous image. Finally the POC method is again to apply to the two maps for finding out the shift parameters △x. The same procedure is repeated to obtain the other two directional shift △y and △z. The rigid registration is completed by the parameter of rotation and displacement alignment.

2.3 Detection of the large tumors by subtraction of two maps

In order to detect the tumor region efficiently and decrease the searching time by SGDS filter, the size of tumor is separated into two categories: larger or less than 10 mms in radius. The mean intensity and standard deviation of the liver region that derived from edge map of liver *E1* is firstly calculated as a reference threshold value for binarization, from which the gray map of *G1* is extracted on the non-contrast phase images. Because the tumor region is included in an edge liver map *E2* on portal venous phase images but excluded in a gray liver map *G1*, the initial tumors are derived from the subtraction of *E2* and *G1* as shown in Fig. 3. Finally, the tumor region with radius larger than 10 mms is identified from the candidates by using the features of circularity and volume.

2.4 Detection of small tumors by spherical gray-level differentiation searching (SGDS) filter

Small tumors are often misdetected due to its small size and sometimes being vanished by morphology processing. In addition, the boundary between tumor and liver are always very subtle and difficult to detect draw an explicit line to separate them. However there are different average gray values in these two regions. Based on the gray-level differentiation, we propose a spherical gray-level differentiation searching (SGDS) filter that searches a spherical area with a certain differentiation value and provide a sphere-like edge score image. The structure of our proposed SGDS filter is shown in Fig.4, where pixel in red is a kernel region, arrows indicate the 8 searching directions.

An average gray value is firstly calculated within a 3X3 kernel region as a substratum by which pixels alone the 8 searching direction are subtracted. If the subtraction value on a point is higher than the threshold t, then stopping searching at this direction and the point is marked as edge point (yellow or blue point in Fig. 4). The white circle (spherical area) is then made to include maximum edge points near the circle, from which the distance to each 8 points D_i is calculated. For a sphere like tumor ROI, D_i is small and less than the threshold d, and the score number is added with 1 in each 8 points. On the contrary, a linear shape vessel ROI has a large $D_i > d$, and no score number is changed in

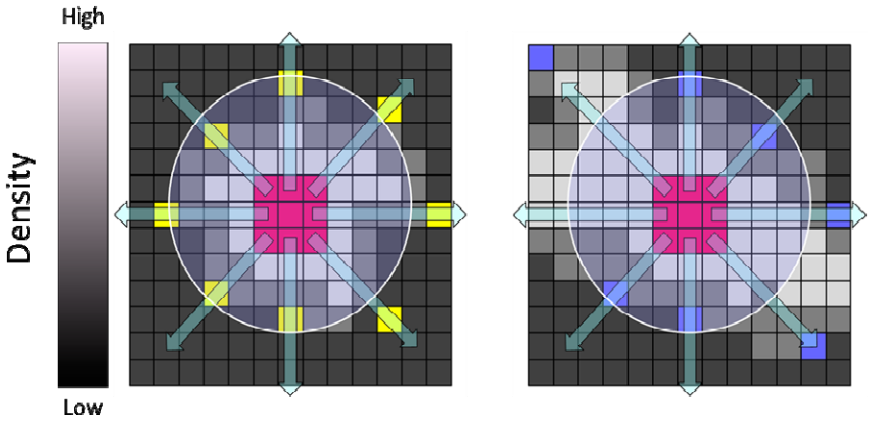

(a) (b)

Figure 4. The structure of spherical gray-level differentiation searching (SGDS) filter consists a kernel region (3X3 red pixels), 8 searching directions (arrows), spherical searching area (within the white circle). (a) is a tumor ROI marked by yellow points in 8 searching directions with score +1, and 8 blue points in (b) is a vessel ROI with score +0.

each 8 points. In case of detecting small tumor, if no point in searching direction with a 50 pixel lengths satisfy the condition *t*, this searching is stopped. Finally a score image is obtained by scanning the whole CT images. A label is regarded as a tumor candidate if the subtraction result of two maps is with value 1 while the score on its edge is higher than 20 by SGDS filter.

2.5 Eliminating the FPs

The final metastatic liver tumor is extracted on the portal venous phase images. A tumor region is firstly identified from the candidates by the features of circularity, volume and the intensity of a label. Further FPs is eliminated by using texture feature-contrast, which is calculated from gray-level co-occurrence matrix (GLCM) [13] with parameter r=1, θ={0°, 45°, 90°, 135}. The contrast of TP tumor has low value in all directions, but a FP has high contrast value in a certain direction. The threshold value of above 4 features is determined by rule-base method using 10 random CT cases.

3. RESULTS AND DISCUSSIONS

12 normal cases and 25 cases are used to test the performance of our algorithm. The registration by two sequenced phases on all the cases is successful according to a visual evaluation. Figure 2 shows a registration result of the liver edge maps on unenhanced (a) and portal venous phase (b) images with a largest liver slice. After log-polar transformation the log-polar Fourier spectrum images are generated as shown in (c) and (d), respectively. Calculating the cyclical shift along horizontal axis between (c) and (d) by POC method, $\theta = 9^{o}$ is calculated as the rotation angle from which a registered image (e) is derived, corresponding to image (a). Rotation turning into shift problem enables the POC method to be used twice to solve both rotation and shift registration. In addition, calculating the translational shift along vertical axis between (c) and (d) can provide image scaling parameter. Therefore, shift, rotation and scaling invariance is possible by combining the log-polar transformation and POC method.

A large tumor candidate with radius more than 50 pixels as shown in Fig.3 is extracted by using the subtraction result of *E2* and *G1* images. Because the tumor on non-contrast CT images always has a homogeneous intensity distribution, gray map *G1* can exclude the tumor region clearly. Its subtraction performance is better than using that of gray map *G2*, as some tumor in portal venous phase image may have a fibrous capsule around its edge. It is also possible to use subtraction result of *E1* and *G1* images to detect additional TPs as some tumors may be observed on non-contrast phase

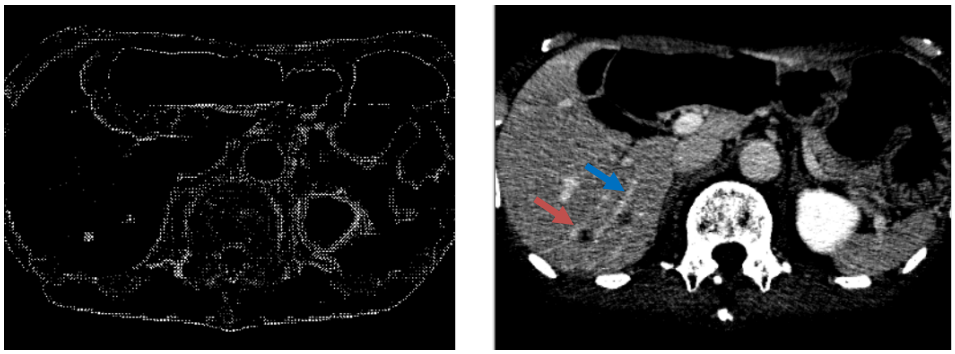

(a) (b)

Figure 5. The result of the output image by SGDS filter (a) is effective to detect spherical shape tumor corresponding to its original CT images (b) with the very low scores on linear component.

but invisible on portal venous phase. The same situation is occurred on *E2* and *G2* that means our method can be modified to use in a single phase image.

We notice that all the spherical candidates are with high scores on its edge and line-structured components like vessels are with low scores after scanning each pixel on the whole image by SGDS filter. Figure 4(a) contains a TP tumor in ROI and yellow points in are the target point where is the location of stopping searching with score +1, and the blue points in Fig. 4(b) are the points where stop searching without score increasing in a vessel pattern.

A result of the score image scanned by SGDS filter is shown in Fig. 5(a). A red arrow pointed spherical shape tumor in original CT image Fig. 5(b) has high scores at the corresponding position on (a), which regarded as one candidate. On the contrary, a blue arrow pointed linear shape vessel has low scores and invisible on (a). Our method is effective for detecting TPs while keeping low FPs rate in the first step. It is found that the small tumor has low score at edges, and therefore it is important to select a proper threshold value so as to keep these small TP tumors into detectable candidates.

Figure 6 is a comparison performance of edge detection by using SGDS filter and LoG [14] filter on a simulation image with noisy background and an unclear sphere target. The result detected by SGDS filter on Fig. 6(b) demonstrates its ability not to be effected by surround noise if the searching subtraction threshold value is lower than noise. SGDS is also found to have the advantage of extracting objects with unclear edge than LoG filter.

On the first detection of 12 normal cases and 25 cases with 44 metastatic liver tumors, 92.7% of TPs are detected with 13.8 FPs per case. After applying the 4 features to eliminate FPs, the accuracy of our algorithm yields 86.7% of TPs rate with 2.5 FPs per case, that implies the effective of our CAD system.

Other types of liver tumor such as Cyst or hemengioma also can be extracted by this method. As the image finding on

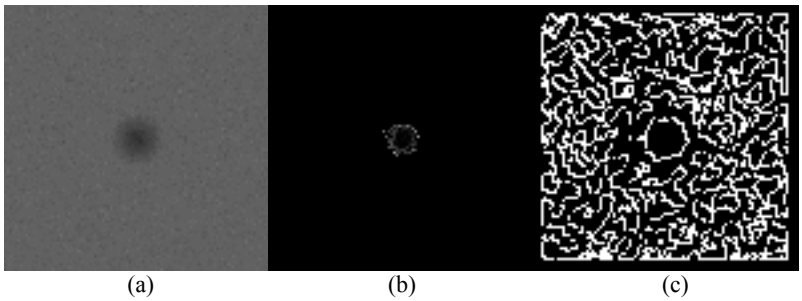

(a) (b) (c)

Figure 6. The comparisons of the performance by SGDS filter (b) and LoG filter (c) on a simulation images (b) with noisy background and an unclear sphere.

CT among different tumors is quite different both on intensity or shape on two phase CT images, we could classify tumors into benign and malignant according to different attenuation values from other phase image that is well registered by POC method. It is well established that hemangiomas are identified by their characteristic peripheral contrast enhancement rather than by the magnitude of their signal intensity. In addition, the enhancement pattern of metastases is highly dependent on the type and vascularity of the primary cancer. The integration of such additional information into the classification will be the next step in this study.

4. CONCLUSIONS

This paper presents our novel method of using liver maps to the registration of two CT phases images. POC can be used to detect shift on two special images and rotation on two power spectrum images. We also describe our proposed SGDS filter for detecting the spherical candidates and constrain linear components. The result demonstrates that the POC is a robust method for the liver registration, and our proposed (SGDS) filter is effective to detect spherical shape tumor on CT images. It is expected that our CAD system could useful in clinical practice.

5. ACKNOWLEDGMENTS

The works are supported by a grant for the Knowledge Cluster Creation Project from the Ministry of Education, Culture, Sports, Science and Technology, Japan, grants of Grant-in-Aid for Scientific Research (KAKENHI) from the Ministry of Education, Culture, Sports, Science and Technology, Japan, a grant from Ministry of Health, Labour, and Welfare, Japan, under a Grant-In-Aid for Cancer Research, and a grant from Ministry of Economy, Trade and Industry, Japan.

Parts of the MDCT data used in this study are provided by National Cancer Center Hospital East, Chiba and National Kyushu Cancer Center, Kyushu. The authors would like to thank Shigeru Nawano and Kenji Shinozaki for their radiological interpretation advices and great contribution to this paper.

The author X. Zhang would like to thank the research support from the National Natural Science Foundation of China (No. 60863014 & 60762001); in part by the Program to Sponsor Teams for Innovation in the Construction of Talent Highlands in Guangxi Institutions of Higher Learning; in part by a research foundation project of the Guangxi Ministry of Education (No. 200810MS048).

REFERENCES

[1] H. El-Serag, and A. Mason, "Rising incidence of hepatocellular carcinoma in the United States", *N. Engl. J. Med.* **340**, 745–750 (1999).

[2] X. Zhang, X. Zhou, T. Hara, et al., "Computer-aided detection and diagnosis on hepatic MR and CT images", International Forum of Computer Science and Technology Application (IFCSTA), 323-326 (2010).

[3] S. Miotani, X. Zhang, M. Kanematsu, et al., "A novel approach to measure the elasticity of liver based on liver deformations on MR tagging image", *Radiological Society of North America Scientific Assembly and Annual Meeting Program, Radiological Society of North America (RSNA)*, 118 (2010).

[4] X. Zhang, M. Kanematsu, H. Fujita, et al., "Application of an artificial neural network to the computer-aided differentiation of focal liver disease in MR imaging", Springer, *Radiological Physics and Technology* **2(2)**, 175-182 (2009).

[5] H. Kato, M. Kanematsu, X. Zhang, et al., "Computer-aided diagnosis of hepatic fibrosis: preliminary evaluation of MRI texture analysis using the finite difference method and an artificial neural network", *AJR* **189**, 117-122 (2007).

[6] T. Tajima, X. Zhang, T. Kitagawa, M. Kanematsu, X. Zhou, T. Hara, H. Fujita, R. Yokoyama, H. Kondo, and H. Hoshi, "Computer-aided detection (CAD) of hepatocellular carcinoma on multiphase CT images", *Proc. of SPIE Medical Imaging 2007: Computer-Aided Diagnosis* **6514**, 65142Q-1-65142Q-10 (2007).

[7] R. Xu, Y. Chen, S. Tang, et al., "3D non-rigid image registration algorithm for MR-guided microwave thermo-coagulation of liver tumors", *Medical Imaging Technology* **25(4)**, 261-276 (2007).
[8] M. Freiman, Y. Edrei, E. Gross, et al., "Liver metastases early detection using fMRI based statistical model", *Proc. of the 5th IEEE Int. Symp. on Biomedical Imaging: From Nano to Macro*, 584-587 (2008).
[9] X. Zhang, T. Tajima, T. Kitagawa, M. Kanematsu, X. Zhou, T. Hara, H. Fujita, R. Yokoyama, H. Kondo, H. Hoshi. "Segmentation of liver region with tumorous tissues", *Proc. of SPIE Medical Imaging 2007: Image Processing* **6512**, 651235-1-651235-9 (2007).
[10] X. Zhang, W. Li, H. Fujita, et al. "Automatic segmentation of hepatic tissue and 3D volume analysis of cirrhosis in multi-detector row CT scans and MR imaging", *IEICE Trans. Inf. & Syst.* **E87-D(8)**, 2138-2147 (2004).
[11] Jia-Zhu Wangyx, Lawrence E Reinsteiny, Joseph Hanleyz and Allen G Meeky. "Investigation of a phase-only correlation technique for anatomical alignment of portal images in radiation therapy", *Phys. Med. Biol.* **41**, 1045-1058 (1996).
[12] S. Pereira, JJK Ó Ruanaidh, F. Deguillaume, G. Csurka, and T. Pun, "Template based recovery of Fourier-based watermaks using log-polar and log-log maps," *Proc. IEEE Int. Conf. on Multimedia Computing and Systems*, 870-474 (1999).
[13] R. Haralick, K. Shanmugam, and I. Dinstein, "Texture features for image classification", *IEEE Trans. Sys. Man Cybern* **Vol. SMC-3-6**, 610-621 (1973).
[14] D. Marr and E. Hildreth, "Theory of edge detection," *Proc. Royal Society of London* **B207**, 187–217 (1980).